



HAL
open science

Undifferenced ambiguity resolution applied to RTK

Sébastien Carcanague, Olivier Julien, Willy Vigneau, Christophe Macabiau

► **To cite this version:**

Sébastien Carcanague, Olivier Julien, Willy Vigneau, Christophe Macabiau. Undifferenced ambiguity resolution applied to RTK. ION GNSS 2011, 24th International Technical Meeting of The Satellite Division of the Institute of Navigation, Sep 2011, Portland, United States. pp 663-678. hal-01022490

HAL Id: hal-01022490

<https://enac.hal.science/hal-01022490>

Submitted on 29 Sep 2014

HAL is a multi-disciplinary open access archive for the deposit and dissemination of scientific research documents, whether they are published or not. The documents may come from teaching and research institutions in France or abroad, or from public or private research centers.

L'archive ouverte pluridisciplinaire **HAL**, est destinée au dépôt et à la diffusion de documents scientifiques de niveau recherche, publiés ou non, émanant des établissements d'enseignement et de recherche français ou étrangers, des laboratoires publics ou privés.

Undifferenced Ambiguity Resolution Applied to RTK

Sébastien CARCANAGUE, *M3SYSTEMS/ENAC, France*

Olivier JULIEN, *ENAC, France*

Willy VIGNEAU, *M3SYSTEMS, France*

Christophe MACABIAU, *ENAC, France*

BIOGRAPHIES

Sébastien CARCANAGUE graduated as an electronic engineer in 2009 from the ENAC (Ecole Nationale de l'Aviation Civile) in Toulouse, France. Since 2009, he is a PhD student at the signal processing lab of ENAC and M3SYSTEMS working on precise positioning algorithm in constrained environments.

Olivier Julien is a researcher/lecturer at the signal processing laboratory of ENAC (Ecole Nationale de l'Aviation Civile – French Civil Aviation University), Toulouse, France. His research interests are GNSS receiver design, GNSS multipath and interference mitigation and GNSS interoperability. He received his engineer degree in 2001 in digital communications from ENAC and his PhD in 2005 from the Department of Geomatics Engineering of the University of Calgary, Canada.

Willy Vigneau graduated from the “Ecole Nationale Supérieure de l'Aéronautique et de l'Espace” in 1999. He has been in charge of the Radionavigation unit at M3 Systems since 2002, and is especially managing projects related to signal processing studies applied to GPS, EGNOS and GALILEO. He is now technical director of M3 Systems and is following M3 Systems' development on GPS, EGNOS and Galileo algorithms and receivers. Recently, he has been particularly involved in several EGNOS and Galileo related projects as project manager and signal processing engineer.

Christophe MACABIAU graduated as an electronics engineer in 1992 from the ENAC in Toulouse, France. Since 1994, he has been working on the application of satellite navigation techniques to civil aviation. He received his Ph.D in 1997 and has been in charge of the signal processing lab of ENAC since 2000.

ABSTRACT

The Phase Lock Loops of a GNSS receiver can provide very precise carrier phase measurements that can potentially be used for positioning. However these measurements are inherently ambiguous since they include an unknown integer number of carrier cycles referred to as the carrier-phase ambiguity. To estimate this ambiguity, important biases have to be removed from

carrier phase measurements such as atmospheric delays, satellite clocks and orbits errors... There are two ways to do this: (1) to difference the observables from the user receiver (or rover) with the measurements from a reference receiver that is spatially close in order to remove common biases, (2) to remove the biases directly by either using a linear combination between observables, or estimating them or obtaining their values from an external source. The first technique is the basis for Real-Time Kinematic (RTK) that uses at least 2 receivers to estimate the differenced carrier-phase ambiguities. The second technique is the basis for Precise Point Positioning (PPP) that estimate the receiver coordinates, the zenith tropospheric delay and the carrier-phase ambiguities from an ionosphere-free carrier phase combination using precise ephemeris.

Ambiguities can be estimated either directly as integers if the residual measurement errors are small compared to the carrier wavelength or as floats if this is not the case. Once the ambiguities are estimated correctly, carrier phase measurements can be used as unambiguous measurements and the position can be determined with a very high precision, usually at centimeter-level.

In this paper, it will be shown that estimating undifferenced carrier-phase integer ambiguity using a PPP filter on the reference station can help RTK positioning of a road user.

First, a new technique allowing a seamless switch from RTK positioning to PPP positioning will be presented. The capacity of this technique to keep sub-meter accuracy when the communication link required by RTK technique is no longer available will be underlined for both single-frequency and dual-frequency users.

Secondly, it will be shown that estimating ambiguities on the reference receiver and broadcasting them to the rover can be used to improve the accuracy of the RTK float ambiguity solution, resulting in a higher ambiguity resolution success rate.

1. INTRODUCTION

1.1 PRECISE POSITIONING TECHNIQUES

GNSS precise positioning usually refers to 2 main techniques: Real-Time Kinematic (RTK) and Precise Point Positioning (PPP). Short-baseline RTK has the advantage that it doesn't require precise ephemerides and it usually provides a centimeter-level position in a few epochs [Kubo, et al., 2007]. However, it requires a

spatially close and usually expensive reference station as well as a low-latency wireless communication media. On the contrary, PPP allows a user to estimate its position autonomously, requiring only the use of precise ephemerides and satellite clock model which makes it cost-effective. However, the convergence time to a precise position is usually very long (typically 30 minutes for decimeter-level position [Bisnath, et al., 2009]). Although PPP and RTK are sometimes opposed, they are based on the same principle.

The ambiguities can be estimated either as a float or an integer. They are estimated as float values if biases have not been totally removed in the measurements. It is the case for long-baseline RTK, in which residual tropospheric and ionospheric delays and carrier-phase noise have potentially an amplitude that is larger than half the carrier wavelength. It is also the case for PPP if the satellite clock correction used doesn't correct for satellite hardware delays.

Ambiguities can also be estimated as integer, as it is the case for short-baseline RTK and PPP with ambiguity resolution (PPP-AR). Estimating ambiguities as integers considerably reduce the solution search space, implying a quicker convergence to a precise position provided no other bias are included in the observations. PPP-AR is relatively new and requires the use of specific satellite biases. The reader might refer to [Laurichesse, et al., 2009], [Collins, 2008] and [Ge, et al., 2008] for more details on this technique allowing undifferenced integer carrier-phase ambiguity resolution. The aim of the present paper is to determine how PPP-AR and RTK techniques can be merged and how both technique advantages can be used by a road user.

1.2 ROAD USER ENVIRONMENT ANALYSIS AND SCENARIO UNDER STUDY

GPS receivers have become a mass-market device used by millions of drivers every day. Current positioning accuracy is usually sufficient to lead the way of a car driver into an unknown area. However, stand-alone positioning technique is not precise enough for Advanced Driver Assistance Systems (ADAS). Examples of such systems include lane keeping assistant, anti-collision and automatic control, typically requiring decimeter or even centimeter accuracy, regardless of the environment. It is all the more difficult to use GPS for road users that it experiences a wide range of propagation channels. It goes from a near-clear sky environment on a highway to the low satellite visibility and high multipath environment found in downtown urban canyon.

Environments tackled in this paper are such that carrier-phase observables coming from a minimum of 4 satellites are expected to be available:

- Semi-urban environment that can typically be found on a beltway.
- Rural environment

PPP alone cannot be used by road users due to long initialization or re-initialization time before obtaining a precise position. It is the reason why RTK was chosen as the primary precise positioning technique. The

improvement of RTK in the examined environments will be studied in this paper, for both dual-frequency and single-frequency rover receivers. A short distance baseline will be assumed in the paper, in order to disregard issues related to atmospheric effects.

The next section will describe the challenges associated to RTK positioning in the selected environments.

1.3 CHALLENGES OF RTK POSITIONING FOR ROAD USERS IN STUDIED ENVIRONMENTS

Urban environment are harmful to RTK positioning because of [Kubo, et al., 2007]:

- High multipath on the pseudorange and the carrier phase.
- Frequent cycle slips.
- Frequent loss of lock due to signal blockage and more generally weak satellite geometry.

In order to have an idea of how GPS observations are affected in a semi-urban environment, data was collected on Bordeaux (France)'s beltway with a Septentrio PolarX2 (dual-frequency receiver), during 4 sessions of approximately 1 hour each. Statistics of availability on all sessions were computed and presented on Table 1. It can be seen that carrier-phase availability is generally lower than code pseudorange availability, resulting in weaker satellite geometry. Additionally, it can be denoted that L1 Doppler measurements have a significantly higher availability than L1 carrier phase. Moreover, a study of the time span duration of a loss of lock and the duration between 2 losses of lock was also performed. Results can be found on Figure 1 and Figure 2. It can be deduced that even if cycle slips are corrected, a road user on Bordeaux's beltway has less than 25 seconds to fix the ambiguity of a satellite 70% of the time and less than 50 seconds 90% of the time.

Signal/ Number of satellites	L1	C1	L2	P2	L1 Doppler
> 3	0.915	0.996	0.825	0.829	0.9733
> 4	0.902	0.990	0.793	0.796	0.966
> 5	0.885	0.989	0.750	0.747	0.958
> 6	0.866	0.983	0.682	0.685	0.946
> 7	0.841	0.970	0.589	0.589	0.930

Table 1 Availability statistics of Septentrio PolarX2 1Hz data collected on Bordeaux's beltway during 4 sessions of approximately 1 hour each

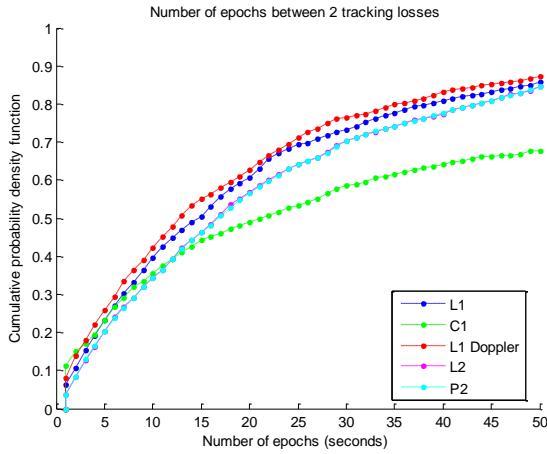


Figure 1 Number of epochs between 2 tracking losses cumulative density function for GPS L1 C/A code, carrier phase and Doppler and L2(P) code and carrier-phase. Data was collected on Bordeaux(France) beltway with a Septentrio PolarX2.

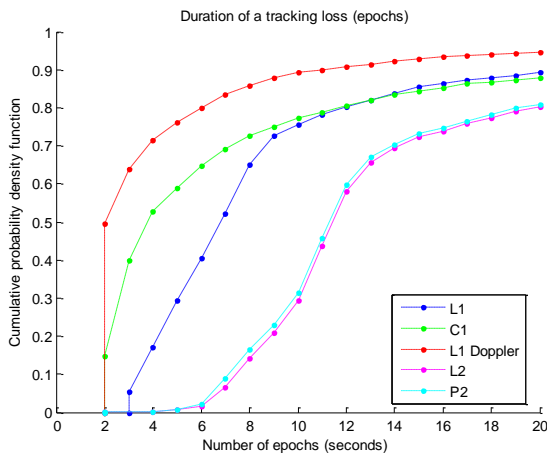


Figure 2 Duration of tracking losses cumulative density function, for GPS L1 C/A code, carrier phase and Doppler and L2(P) code and carrier-phase. Data was collected on Bordeaux(France) beltway with a Septentrio PolarX2.

In rural area, the GPS propagation channel is less restrictive as it usually offers better satellite visibility and less signal blockage. However, cellphone network coverage is worse than in urban area. [Yang, et al., 2010] points out that local tests on UK roads have shown that even on the highway roads, the cell phone network cannot be guaranteed.

1.4 POSSIBLE IMPROVEMENTS BROUGHT BY UNDIFFERENCED AMBIGUITY RESOLUTION ON THE REFERENCE STATION TO RTK FOR ROAD USERS

In this paper, it will be shown that estimating undifferenced carrier-phase integer ambiguity using a PPP filter on the reference station and broadcasting them to the rover can help RTK positioning in the different studied environment.

First, a new technique allowing a seamless switch from RTK positioning to PPP positioning on the rover will be

presented. The capacity of this technique to keep sub-meter accuracy when the communication link required by RTK technique is no longer available will be underlined for both single-frequency and dual-frequency users. Secondly, it will be shown that estimating ambiguities on the reference receiver can be used to reduce the noise and multipath contribution of the reference receiver in the RTK float ambiguity solution, resulting in a higher ambiguity resolution success rate.

2. PRECISE POSITIONING BACKGROUND

2.1 NOTATIONS, MEASUREMENT MODEL AND CLASSIC OBSERVATION COMBINATIONS

Measurement model

In this paper, the following measurement model will be used for code and carrier-phase measurements (in meters):

$$\begin{cases} P_i = \rho + c(dt - dT) + I_i + T + b_{r,P_i} - b_{P_i}^s + m_{P_i} + \varepsilon_{P_i} \\ \phi_i = \rho + c(dt - dT) - I_i + T + b_{r,\phi_i} - b_{\phi_i}^s + N_i \lambda_i + W \lambda_i + m_{\phi_i} + \varepsilon_{\phi_i} \end{cases}$$

where

- i designates the carrier frequency of the signal,
- ρ is the true geometric range between satellite and receiver antenna,
- c is the speed of light,
- dt and dT are the biases associated to receiver and satellite oscillator offset and are irrespective of the signal observed,
- I_i is the delay due to ionosphere on frequency i ,
- T is the tropospheric delay,
- $b_{r,Obs}$ and b_{Obs}^s are the receiver and satellite hardware biases of the code and carrier-phase observations,
- m_{Obs} is observation multipath,
- ε_{Obs} represents remaining errors of the observation,
- λ_i is the wavelength of the signal's carrier i ,
- N_i is the carrier-phase integer ambiguity and
- W is the wind-up effect.

Classic observation combinations

A number of classic combinations exist and are used in differential positioning or in point positioning. Combinations are formed for 3 purposes: ionospheric delay mitigation, wavelength amplification or noise reduction. Although a combination that is widelane, ionosphere-free and low-noise would be highly desirable, it is mathematically impossible [Urquhart, 2009]. Then, classic combinations are a trade-off related to the need of the user. A detailed study of GPS dual-frequency and Galileo triple frequency combinations can be found in [Collins, 1999] and [Henkel, et al., 2007] respectively. The most famous include:

- **Widelane combination.** It consists in differencing the carrier phase observables directly in cycles unit:

$$\phi_{WL} = \left(\frac{\phi_1}{\lambda_1} - \frac{\phi_2}{\lambda_2} \right) \lambda_{WL}$$

$$= \rho + c(dt - dT) + T + I_{WL} + b_{r,\phi_{WL}} - b_{\phi_{WL}}^S + (N_1 - N_2)\lambda_{WL} + \varepsilon_{\phi_{WL}}$$

It creates an observable that has the same geometrical properties than L1 and L2 double differenced observables but with a longer wavelength $\lambda_{WL} = \frac{1}{\left(\frac{1}{\lambda_1} - \frac{1}{\lambda_2}\right)} = 86.1 \text{ cm}$. $N_1 - N_2$ is then called the wide-lane ambiguity.

- **Narrowlane code combination.**

$$P_{NL} = \left(\frac{P_1}{\lambda_1} + \frac{P_2}{\lambda_2}\right) \cdot \lambda_{NL} = \rho + c(dt - dT) + T + I_{WL} + b_{r,P_{NL}} - b_{P_{NL}}^S + \varepsilon_{P_{NL}}$$

Assuming P_1 and P_2 have similar level of noise, P_{NL} is $\sqrt{\left(\frac{\lambda_{NL}}{\lambda_1}\right)^2 + \left(\frac{\lambda_{NL}}{\lambda_2}\right)^2} \approx 0.71$ less noisy than P_1 . The ionospheric delay of the widelane carrier-phase equals the ionospheric delay of the narrowlane code [Banville, et al., 2008].

- **Melbourne-Wübbena combination.** This combination uses the widelane phase combination in meters and the narrowlane code combination:

$$\phi_{WL} - P_{NL} = (N_1 - N_2)\lambda_{WL} + b_{r,MW} - b_{MW}^S + \varepsilon_{P_{NL}} + \varepsilon_{\phi_{WL}}$$

This combination is very useful to isolate and solve the widelane ambiguity. The narrow lane combination reduces the code noise.

- **Ionosphere-free combination.** It consists in removing the first order of the ionospheric delay, while keeping the other effects unchanged. For dual frequency L1/L2 code measurements:

$$P_{IF} = \alpha P_1 - \beta P_2 = \rho + c(dt - dT) + T + b_{r,P_{IF}} - b_{P_{IF}}^S + \varepsilon_{P_{IF}}$$

where $\alpha = \frac{f_1^2}{f_1^2 - f_2^2} = 2.546$ and $\beta = \frac{f_2^2}{f_1^2 - f_2^2} = 1.546$

The same combination can be formed with carrier-phase observables:

$$\phi_{IF} = \alpha \phi_1 - \beta \phi_2 = \rho + c(dt - dT) + T + \alpha N_1 \lambda_1 - \beta N_2 \lambda_2 + W \lambda_{NL} + b_{r,\phi_{IF}} - b_{\phi_{IF}}^S + \varepsilon_{\phi_{IF}}$$

- **GRAPHIC (GRoup And Phase Ionospheric Correction):**

$$\frac{P_i + \phi_i}{2} = \rho + c(dt - dT) + T + N_i \frac{\lambda_i}{2} + W \frac{\lambda_i}{2} + b_{r,\frac{P_i + \phi_i}{2}} - b_{\frac{P_i + \phi_i}{2}}^S + \varepsilon_{\frac{P_i + \phi_i}{2}}$$

This combination is ionosphere-free but ambiguous. The noise level is half the code noise, which is around 6 times less than ionosphere-free code combination.

Satellite clock and orbit correction model

In order to remove the satellite clock bias and satellite hardware bias, corrections are applied to the measurements by the user. These available corrections are related to one specific combination of observations and corrects for both the satellite clock and the satellite hardware bias for this combination. For example, the satellite clock correction transmitted within the navigation message includes the satellite clock and the satellite

hardware bias corresponding to the $P_1 P_2$ ionosphere-free code combination. This correction can be expressed as $dT + \widehat{b_{P_{IF}}^S}$. As a consequence, when applying directly the satellite clock correction included in the navigation message:

$$P_{IF} + dT + \widehat{b_{P_{IF}}^S} = \rho + cdt + T + b_{r,P_{IF}} + m_{P_{IF}} + \varepsilon_{P_{IF}}$$

If a single-frequency user applies the broadcasted satellite clock directly, a satellite bias $b_{P_{IF}}^S - \widehat{b_{P_{IF}}^S}$ will remain:

$$P_1 + dT + \widehat{b_{P_{IF}}^S} = \rho + cdt + I_1 + T + b_{r,P_1} - b_{P_1}^S + b_{P_{IF}}^S + m_{P_1} + \varepsilon_{P_1}$$

In order to obtain an unbiased position, a correction called ‘‘Time Group Delay (TGD)’’ broadcasted in the navigation message has to be applied ($T_{GD} = b_{P_{IF}}^S - \widehat{b_{P_{IF}}^S}$):

$$P_1 + dT + \widehat{b_{P_{IF}}^S} + \widehat{T_{GD}} = \rho + cdt + I_1 + T + b_{r,P_1} + m_{P_1} + \varepsilon_{P_1}$$

It can be deduced that $\widehat{T_{GD}} = b_{P_{IF}}^S - \widehat{b_{P_{IF}}^S}$

PPP-AR satellite clock correction corrects for both the satellite clock delay and the satellite hardware bias for the ionosphere-free phase combination. It is thus equivalent to $dT + \widehat{b_{\phi_{IF}}^S}$. This means that:

$$\phi_{IF} + dT + \widehat{b_{\phi_{IF}}^S} = \rho + cdt + T + \alpha N_1 \lambda_1 - \beta N_2 \lambda_2 + W \lambda_{NL} + b_{r,\phi_{IF}} + \varepsilon_{\phi_{IF}}$$

Finally, satellite orbit corrections are estimated together with satellite clock corrections. Therefore, it is expected that satellite clock corrections are heavily correlated with orbit radial error. Then, it is important to use orbits and satellite clock from a same source of corrections (broadcasted message, IGS product or PPP-AR products) and not to mix corrections coming from different sources.

2.2 UNDIFFERENCED INTEGER AMBIGUITY RESOLUTION ON THE REFERENCE RECEIVER

Double differenced carrier-phase ambiguities can be easily isolated to integer values. Nonetheless, undifferenced ambiguities in traditional PPP absorb the satellite hardware bias and lose their integer properties. To estimate the undifferenced L1 ambiguities as an integer, a method is proposed in [Laurichesse, et al., 2009]. It is based on the use of clock products that keep the integer property of the narrowlane ambiguity in the ionosphere-free carrier phase combination. To summarize, it is performed in 4 steps:

- **Estimation of the widelane ambiguities.** This step is performed by subtracting Melbourne-Wübbena satellite biases from the Melbourne-Wübbena combination and averaging over a time window (usually 10 minutes [Laurichesse, et al., 2009]).

- **Formation of the ionosphere-free carrier phase combination and application of PPP-AR satellite clock corrections**, i.e.:

$$\phi_{IF} + dT + \widehat{b}_{\phi_{IF}}^s = \rho + cdt + b_{r,\phi_{IF}} + T + \alpha N_1 \lambda_1 - \beta N_2 \lambda_2 + \varepsilon_{\phi_{IF}}$$

- **Removal of widelane ambiguities**, i.e.

$$\begin{aligned} \phi_{IF} + dT + \widehat{b}_{\phi_{IF}}^s - \beta N_{WL} \\ = \rho + cdt + b_{r,\phi_{IF}} + T + N_1 \lambda_{NL} + \varepsilon_{\phi_{IF}} \end{aligned}$$

with $N_{WL} = N_1 - N_2$ and $\lambda_{NL} = \frac{\lambda_1 \lambda_2}{\lambda_1 + \lambda_2} = 10.7 \text{ cm}$

- **PPP-processing to determine the integer narrow-lane ambiguities**. Effects affecting the above pseudorange have to be accurately modeled and removed. The integer narrow-lane ambiguity resolution involves estimating:
 - the receiver clock term ($cdt + b_{r,\phi_{IF}}$),
 - the zenith tropospheric delay, and
 - the integer ambiguities are estimated in a Kalman filter.

The required PPP-AR products can be obtained from different sources. The CNES/CLS IGS center is providing both the satellite clock bias and the Melbourne-Wübbena satellite biases for post-processing purposes (GRG products freely available on the IGS website) [Perosanz, et al., 2009]. Recently, PPP-AR products have been available in real-time via Ntrip streams within the PPP-Wizard project [CNES, 2011].

3. INSTANTANEOUS FIXING OF PPP AMBIGUITIES USING RTK

In RTK processing, observations from the reference station have to be broadcasted very frequently to the user receiver. Indeed, the time correlation of atmospheric errors is relatively short [Olynik, 2002]. If the age of the correction is too old, the error will not be removed or only partially which will reduce the accuracy of the solution. Even if the tracking of the rover receiver is continuous, i.e. the carrier phase ambiguities of the rover receiver remain the same, the accuracy will drop and a standard procedure is to switch to classic single point positioning. In RTKLib [Takasu, 2009], an open-source RTK software, default configuration switches from RTK to single point positioning if the age of the last reference receiver observable is older than 30 seconds.

A first idea would be to run a PPP filter in parallel of the RTK processing, to obtain a high level of precision as soon as RTK is unavailable. However, it has different drawbacks:

- The precision of the PPP software would rely on previous epochs which can be a problem if the rover was in a difficult environment a few minutes prior to the communication link outage.
- It is computationally heavy.
- Although using the RTK solution to constrain the position would be sufficient to initialize the

PPP software, fixing each ambiguity provides a more redundant information.

The aim of the technique presented herein is an instantaneous PPP ambiguities initialization using only the last single-epoch RTK ambiguities available. The PPP software can then be used to keep a high level of precision as long as the rover carrier-phase tracking remains continuous, without requiring a data link.

3.1 APPLICATIONS OF THE ALGORITHM

The idea of the algorithm is to use the last available data from the reference station to initialize a PPP filter and to keep a high level of accuracy autonomously, i.e. without receiving data from any reference station. A first application to this algorithm would be to cope with a loss of the communication link. Currently, most Network-RTK services are implemented on the commercial cell-phone network services. Tests in the UK have shown that even on the highway, the data cell phone network cannot be guaranteed [Yang, et al., 2010].

Secondly, this method could be applied to reduce the bandwidth resource (data rate) of the RTK corrections in the case of a satellite based NRTK service for example, transmitting data of each station every 5 minutes through a one-way data communication link for example. The accuracy would be maintained between 2 broadcasts reference receiver data using the technique described below and an efficient cycle slip correction method ([Banville, et al., 2009]...).

Finally the correspondence between the rover ambiguities obtained via a PPP filter and a RTK software introduced in this paper could be used for validation purpose. Dual-frequency PPP ambiguity resolution is mainly affected by satellite clock and orbit error while RTK is mainly affected by residual tropospheric and ionospheric delays. Checking that ambiguities correspond between the 2 techniques could be an interesting way to validate the ambiguities.

3.2 DESCRIPTION OF THE ALGORITHM

The algorithm is as such:

First step: Determination of L1 undifferenced carrier-phase ambiguities on the reference receiver.

To do so, reference receiver carrier phase observations are processed in a PPP software receiver together with real-time products as described in 2.2. An open-source software receiver is freely available on the website of the PPP-Wizard project [CNES, 2011]. This software includes a PPP processor capable of interpreting the real-time stream broadcasted by CNES. This stream includes all the correction needed for integer PPP. A small modification of the sources can be made so that the software outputs the N_1 ambiguities in real-time.

Once the N_1 ambiguities are fixed, they can be subtracted from the L1 carrier phase observables to form unambiguous observables similar to code pseudoranges. Following notations from 4., unambiguous carrier phase

measurements will be referenced as $\bar{\Phi}$ in the following algorithm description.

Second step: Resolution of double-differenced ambiguities using RTK technique

The next step is to estimate the double-differenced carrier phase ambiguities. Different techniques can be used as the LAMBDA technique or the LMS technique [Enge, et al., 2nd Edition]. They can be roughly summarized as:

- A reference satellite i is chosen. It is usually a high elevation satellite, tracked by both stations
- The double-differenced carrier phase ambiguities are estimated using any integer ambiguity resolution technique (it is assumed that the residual atmospheric delays are negligible). The double differenced ambiguity can be decomposed as such:

$$\Delta \nabla N = \nabla N^{\text{rov}} - \nabla N^{\text{ref}} = {}^j N^{\text{rov}} - {}^i N^{\text{rov}} - ({}^j N^{\text{ref}} - {}^i N^{\text{ref}})$$

In our algorithm, the unambiguous carrier-phase measurements of the reference receiver are used instead of the raw carrier phase measurements:

$$\Delta \nabla \Phi = \nabla \Phi^{\text{rov}} - \nabla \bar{\Phi}^{\text{ref}}$$

Since ${}^i N^{\text{ref}} = {}^i N^{\text{ref}}$ can be considered as null as the carrier phase measurements of the reference receiver are no longer ambiguous, the double differenced ambiguities only include the rover ambiguities:

$$\Delta \nabla N^j = {}^j N^{\text{rov}} - {}^i N^{\text{rov}}$$

Third step: Instantaneous initialization of rover ambiguities in the point positioning model

Now, let's assume that the communication link has been lost and that the last data from the reference receiver is older than 30 seconds. The carrier-phase ambiguities, should remain the same as long as the tracking is continuous. Instead of switching to single-point positioning, the RTK rover ambiguities can be used to improve the accuracy of the solution. First, the carrier phase observations on L1 on the rover are:

$$\begin{cases} {}^1 \phi = {}^1 \rho + c(dt - {}^1 dT) - {}^1 I_1 + {}^1 T + {}^1 N_1 \lambda_1 + {}^1 W \lambda_1 + b_{r, {}^1 \phi} - b_{i, {}^1 \phi}^s + \varepsilon_{{}^1 \phi} \\ \dots \\ {}^i \phi = {}^i \rho + c(dt - {}^i dT) - {}^i I_1 + {}^i T + {}^i N_1 \lambda_1 + {}^i W \lambda_1 + b_{r, {}^i \phi} - b_{i, {}^i \phi}^s + \varepsilon_{{}^i \phi} \\ \dots \\ {}^n \phi = {}^n \rho + c(dt - {}^n dT) - {}^n I_1 + {}^n T + {}^n N_1 \lambda_1 + {}^n W \lambda_1 + b_{r, {}^n \phi} - b_{i, {}^n \phi}^s + \varepsilon_{{}^n \phi} \end{cases}$$

With the subscript on the right indicating the carrier frequency, the superscript on the left indicating the satellite number, i the reference satellite and n the number of satellites.

Subtracting the following vector (composed of the reference receiver single-differenced ambiguities), which is null for the reference satellite and equal to the previous RTK ambiguities for the other satellite, to the carrier phase observations:

$$\begin{cases} \bar{{}^1 \phi} = {}^1 \phi - \Delta \nabla N^1 = {}^1 \phi - ({}^1 N - {}^i N) \\ = {}^1 \rho + c(dt - {}^1 dT) - {}^1 I_1 + {}^1 T + {}^i N_1 \lambda_1 + {}^1 W \lambda_1 + b_{r, {}^1 \phi} - b_{i, {}^1 \phi}^s + \varepsilon_{{}^1 \phi} \\ \dots \\ \bar{{}^i \phi} = {}^i \phi - 0 \\ = {}^i \rho + c(dt - {}^i dT) - {}^i I_1 + {}^i T + {}^i N_1 \lambda_1 + {}^i W \lambda_1 + b_{r, {}^i \phi} - b_{i, {}^i \phi}^s + \varepsilon_{{}^i \phi} \\ \dots \\ \bar{{}^n \phi} = {}^n \phi - \Delta \nabla N^n = {}^n \phi - ({}^1 N - {}^i N) \\ = {}^n \rho + c(dt - {}^n dT) - {}^n I_1 + {}^n T + {}^i N_1 \lambda_1 + {}^n W \lambda_1 + b_{r, {}^n \phi} - b_{i, {}^n \phi}^s + \varepsilon_{{}^n \phi} \end{cases}$$

The ambiguities associated to each satellite have been eliminated from the L1 carrier-phase measurements, and the reference satellite ambiguity ${}^i N_1$ is now common to all satellites and can be lumped into the receiver clock/hardware bias term. The observables are not ambiguous anymore and can be used for positioning.

Fourth step: Using the unambiguous carrier-phase on the rover for point positioning: dual-frequency and single-frequency case

Now that the carrier-phase observations have been turned into precise pseudoranges, they can be used for positioning. In order to obtain a precise position from these low noise and multipath measurements, all the errors affecting these pseudoranges have to be removed. Orbit error, satellite clock error and tropospheric delay should be almost completely eliminated as long as precise ephemerides are used and tropospheric delay is estimated in the positioning model. However, the ionospheric delay has to be removed. A dual-frequency user can directly use the L1 rover ambiguities in the ionosphere-free carrier-phase measurements to obtain instantly a decimeter-level position. However, it is more difficult for a single-frequency user. There are 2 ways to remove the ionospheric delay:

- Using a code and carrier-phase combination. The GRAPHIC combination can be used:

$$\begin{aligned} \frac{\bar{\Phi}_1 + P_1}{2} &= \rho + c(dt - dT) + T + W \frac{\lambda_1}{2} + b_{r, \frac{\bar{\Phi}_1 + P_1}{2}} - b_{\frac{\bar{\Phi}_1 + P_1}{2}}^s \\ &\quad + m_{\frac{\bar{\Phi}_1 + P_1}{2}} + \varepsilon_{\frac{\bar{\Phi}_1 + P_1}{2}} \end{aligned}$$

Note that $b_{r, \frac{\bar{\Phi}_1 + P_1}{2}}$ includes the reference satellite carrier-phase ambiguity ${}^i N_1 \lambda_1$.

It has the advantage to be ionosphere-free and to divide the code noise and multipath error influence on the position by 2. However, the bias $b_{\frac{\bar{\Phi}_1 + P_1}{2}}^s$ has to be determined.

- Using broadcasted ionospheric corrections or SBAS corrections, applied to the unambiguous carrier phase:

$$\bar{\Phi}_1 = \rho + c(dt - dT) + T - I_1 + W \lambda_1 + b_{r, \Phi_1} - b_{\Phi_1}^s + m_{\Phi_1} + \varepsilon_{\Phi_1}$$

This solution has the advantage that it doesn't use code measurement. Then the accuracy of the estimated position would not be deteriorated by code multipath and noise. However, the final accuracy of the position is highly dependent on

the precision of the ionospheric corrections.

Moreover, $b_{\Phi_1}^s$ has to be estimated.

Both techniques need specific bias estimation to obtain a precise position. The bias estimation will be described in the next section.

3.3 SATELLITE BIAS ESTIMATION

The observables that are proposed to be used in the previous section contain satellite biases that will not be mitigated when applying broadcasted or IGS satellite clock. These biases will be specific to each satellite. From our own experience, they can have a meter-level amplitude. Then, these biases have to be isolated and eliminated in order to obtain an unbiased position. To do so, it has been seen in 2.1 that different satellite clock corrections including different satellite biases can be used. In order to simplify notations, a reference satellite clock is chosen in the next section.

REFERENCE SATELLITE CLOCK DEFINITION

The aim of the studied algorithm is to keep a precise position when the data of the reference station is no longer available. Considering that the reference station is equipped with redundant hardware and software, a probable cause of an unavailability of the reference station data is a loss of the communication link on the rover due to GSM network unavailability or modem malfunctioning. Then, the use of PPP-AR precise ephemerides that requires a connection to a distant server would certainly not be possible. That is why the reference satellite clock will be referred to the P_1P_2 ionosphere-free combination in the following work. It is the observable combination directly corrected by IGS or navigation message satellite clocks.

3.4 DUAL-FREQUENCY CASE: POSITIONING WITH UNAMBIGUOUS IONOSPHERE-FREE COMBINATION

Once the widelane and the narrowlane ambiguities are determined on the dual-frequency rover, the unambiguous ionosphere-free combination can be formed and used for positioning. If the rover has access to the PPP-AR products used by the reference station, no bias estimation is required. If the user has to switch to IGS/broadcasted ephemeris, a bias has to be corrected. It can simply be obtained at every epoch by differencing the PPP-AR satellite clock correction used on the reference receiver with the IGS/broadcasted ephemeris. To take into account any difference in the satellite clock that would have been lumped into radial orbit error, the geometric ranges obtained using the 2 sets of products are also differenced:

$$b_{P_{1F}-\Phi_{1F}}^s = dT + \widehat{b}_{P_{1F}}^s + \widehat{\rho}_{P_{1F}} - dT + \widehat{b}_{\Phi_{1F}}^s - \widehat{\rho}_{\Phi_{1F}}$$

where $\widehat{\rho}_{P_{1F}}$ and $\widehat{\rho}_{\Phi_{1F}}$ are the geometric range computed with IGS/broadcasted message orbits and PPP-AR orbits respectively.

A plot of the time evolution of $b_{P_{1F}-\Phi_{1F}}^s$ for the different satellite can be found on Figure 3. It is important to denote that only the difference between satellite values is important, since any bias common to all satellite will be

absorbed in the receiver clock estimation. Even if the value of the bias has a clear time evolution, the difference between satellite is relatively stable over a day.

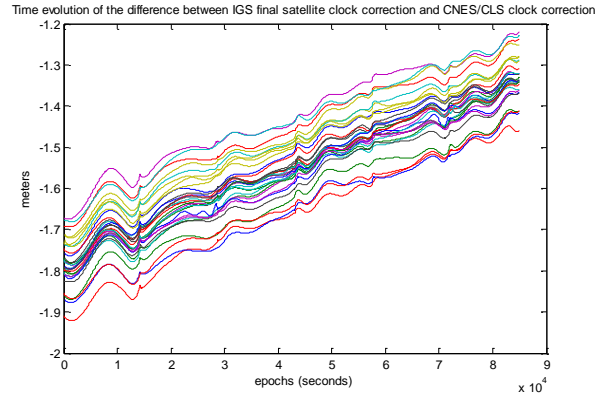


Figure 3 Time evolution of the difference between IGS final satellite clock correction and GRGS satellite clock correction (including orbit satellite radial error). The geometric range is computed using the position of TLSE1 (Toulouse, France). PRN01 (SVN49) is not included.

3.5 SINGLE-FREQUENCY CASE: POSITIONING WITH UNAMBIGUOUS GRAPHIC OBSERVABLES

As described earlier, the unambiguous GRAPHIC combination corrected using the broadcasted satellite clock correction is as such:

$$\frac{\overline{\Phi_1} + P_1}{2} + dT + \widehat{b}_{P_{1F}}^s = \rho + cdt + T + W \frac{\lambda_1}{2} + b_{r, \frac{\Phi_1 + P_1}{2} - P_{1F}} - b_{\frac{\Phi_1 + P_1}{2} - P_{1F}}^s + m_{\frac{\Phi_1 + P_1}{2}} + \varepsilon_{\frac{\Phi_1 + P_1}{2}}$$

Where $\overline{\Phi_1}$ is the unambiguous L1 carrier-phase measurement.

$b_{\frac{\Phi_1 + P_1}{2} - P_{1F}}^s$ has to be mitigated as it is specific to each satellite. Three methods are proposed.

3.5.1 GRAPHIC SATELLITE BIAS ESTIMATION USING P1P2 CODE MEASUREMENTS

Subtracting the P_1P_2 ionosphere-free combination to the unambiguous GRAPHIC combination on the reference station gives:

$$\frac{\overline{\Phi_1} + P_1}{2} - P_{1F} = W \frac{\lambda_1}{2} + b_{r, \frac{\Phi_1 + P_1}{2} - P_{1F}} - b_{\frac{\Phi_1 + P_1}{2} - P_{1F}}^s + m_{\frac{\Phi_1 + P_1}{2}} + \varepsilon_{\frac{\Phi_1 + P_1}{2} - P_{1F}}$$

The satellite phase windup effect can easily be mitigated using a model. To estimate $b_{\frac{\Phi_1 + P_1}{2} - P_{1F}}^s$, a Kalman filter can be used. $b_{\frac{\Phi_1 + P_1}{2} - P_{1F}}^s$ can be considered constant over a day.

No assumption can be made on $b_{r, \frac{\Phi_1 + P_1}{2} - P_{1F}}$ temporal variation as it contains the reference satellite L1 ambiguity of the rover and it will be estimated as a term common to all satellites. Considering the relatively high level of noise and multipath of the P_1P_2 ionosphere-free combination, the estimation of the satellite bias has to use data from a whole satellite pass and from more than one station. For real-time processing, the satellite bias value of

the day before can be used considering the slow temporal variations of the satellite bias experienced by the authors. However, more accurate methods can be used to determine $b_{\frac{\Phi_1+P_1}{2}-P_{IF}}^S$ can be used, as presented in the next 2 sections.

3.5.2 GRAPHIC SATELLITE BIAS ESTIMATION USING PPP-AR PRODUCTS

Instead of using P1P2 code measurements to directly estimate $b_{\frac{\Phi_1+P_1}{2}-P_{IF}}^S$, it can be noticed that $b_{\frac{\Phi_1+P_1}{2}-P_{IF}}^S$ can be decomposed into 2 terms:

$$b_{\frac{\Phi_1+P_1}{2}-P_{IF}}^S = b_{\frac{\Phi_1+P_1}{2}-\Phi_{IF}}^S - b_{P_{IF}-\Phi_{IF}}^S$$

$b_{P_{IF}-\Phi_{IF}}^S$ is a direct by-product of the difference between the 2 clock corrections as shown in 3.4:

$$b_{P_{IF}-\Phi_{IF}}^S = dT + \widehat{b}_{P_{IF}}^S + \widehat{\rho}_{P_{IF}} - dT + \widehat{b}_{\Phi_{IF}}^S - \widehat{\rho}_{\Phi_{IF}}$$

i.e. subtracting the value of the 2 satellite clock corrections (and taking into account the orbit radial error) at any epoch gives the value of $b_{P_{IF}-\Phi_{IF}}^S$.

To obtain $b_{\frac{\Phi_1+P_1}{2}-P_{IF}}^S$ from $b_{P_{IF}-\Phi_{IF}}^S$, $b_{\frac{\Phi_1+P_1}{2}-\Phi_{IF}}^S$ is now needed. It can be obtained by simply averaging the difference between the unambiguous GRAPHIC observable and the unambiguous ionosphere-free carrier phase and removing the wind-up effect, i.e.:

$$\begin{aligned} \frac{\Phi_1 + P_1}{2} - \overline{\Phi}_{IF} &= W \left(\frac{\lambda_1}{2} - \lambda_{NL} \right) + b_{r, \frac{\Phi_1+P_1}{2}-\Phi_{IF}} - b_{\frac{\Phi_1+P_1}{2}-\Phi_{IF}}^S \\ &+ m_{\frac{\Phi_1+P_1}{2}-\Phi_{IF}} + \varepsilon_{\frac{\Phi_1+P_1}{2}-\Phi_{IF}} \end{aligned}$$

The advantage of this method is that the average window to estimate the bias can be much shorter than in 3.5.1 and the impact of code multipath on the bias accuracy will be reduced.

A last method is presented in the next section. It was used in the rest of this work because it can be used on a single-frequency reference receiver, contrary to the 2 previous methods.

3.5.3 GRAPHIC SATELLITE BIAS ESTIMATION DECOMPOSING THE PSEUDORANGE

Another way to estimate $b_{\frac{\Phi_1+P_1}{2}-P_{IF}}^S$ is to use a station with surveyed coordinates and estimated tropospheric delay, i.e. the reference station or any station with a real-time data stream. Then, the computed geometric range and the slant tropospheric delay can be removed from GRAPHIC pseudorange:

$$\begin{aligned} \frac{\overline{\Phi}_1 + P_1}{2} + dT + \widehat{b}_{P_{IF}}^S - \rho - T - W \frac{\lambda_1}{2} \\ = cdt + b_{r, \frac{\Phi_1+P_1}{2}-P_{IF}} - b_{\frac{\Phi_1+P_1}{2}-P_{IF}}^S + m_{\frac{\Phi_1+P_1}{2}} + \varepsilon_{\frac{\Phi_1+P_1}{2}} \end{aligned}$$

$b_{\frac{\Phi_1+P_1}{2}-P_{IF}}^S$ can then be estimated using a Kalman filter that estimates both satellite biases and a term common to all satellites. It is the recommended method to estimate the different biases.

3.6 SINGLE-FREQUENCY CASE: POSITIONING WITH UNAMBIGUOUS CARRIER-PHASE AND IONOSPHERIC CORRECTIONS

It has been seen that the GRAPHIC observable could be used for single-frequency PPP. The second observable that was proposed to be used for positioning was the unambiguous carrier-phase on L1, using broadcasted or IGS clock corrections:

$$\begin{aligned} \overline{\Phi}_1 + dT + \widehat{b}_{P_{IF}}^S &= \rho + cdt - I_1 + T + b_{r, \Phi_1} - b_{\Phi_1-P_{IF}}^S \\ &+ W\lambda_1 + m_{\Phi_1} + \varepsilon_{\Phi_1} \end{aligned}$$

It can be seen that $b_{\Phi_1-P_{IF}}^S$ has to be determined.

Let's decompose it:

$$\begin{aligned} b_{\Phi_1-P_{IF}}^S &= 2 * b_{\frac{\Phi_1+P_1}{2}-P_{IF}}^S - b_{P_{IF}}^S \\ &= 2 * \underbrace{b_{\frac{\Phi_1+P_1}{2}-P_{IF}}^S}_{\text{determined in the previous section}} + T_{GD} \end{aligned}$$

Having $b_{\Phi_1-P_{IF}}^S$ allows any user to use the carrier-phase observable directly for positioning, using broadcasted or IGS ephemerides.

3.7 ACCURACY TEST ON REAL DATA

3.7.1 HARDWARE, SOFTWARE AND SCENARIO DEFINITION

The different PPP initializations have been tested on real data. The reference station was TLSE based in Toulouse, France. The data was collected via a real-time stream and a modification of the software BNC available on the website [CNES, 2011], but it was post-processed. The rover receiver was a uBlox LEA-6T single-frequency receiver, connected to a static antenna on the roof of an ENAC building. The position of the antenna was surveyed on the day of the data collection, using data from a Novatel Propak-G2 dual frequency receiver connected to the same antenna via a splitter and the online PPP software GAPS from the University of New-Brunswick [Leandro, 2009]. The baseline length was approximately 400 meters. L1 carrier-phase ambiguities on the reference receiver were determined using a modified version of BNC. Then, the double-differenced range was determined from the known baseline, and removed from double-differenced carrier-phase to obtain double differenced ambiguities. Finally, the reference receiver ambiguities were removed from the double-differenced ambiguities, to obtain the rover ambiguities as explained in 3.

The position of the antenna was estimated on a single-epoch basis, using L1 C/A code measurements from the uBlox receiver. The result can be found on Figure 4.

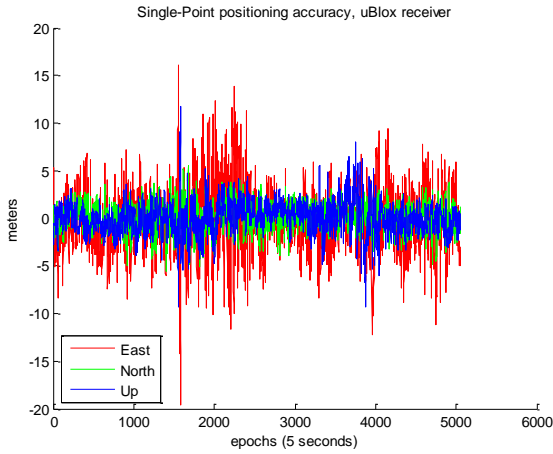


Figure 4 Single point position accuracy, with code measurements from a uBlox LEA-6T, using rapid IGS ephemeris and EGNOS ionospheric corrections. Raw code measurements were used as provided by the uBlox and were weighed by the cosecant function of the elevation angle. Data rate is 1/5 Hz. No assumption was made on the dynamic of the receiver.

It can be seen that raw code measurements have a very high level of noise/multipath and provide a meter level position.

The aim of this part is to determine the type of accuracy that can be expected and if the technique can give better accuracy than stand-alone positioning when the age of the last reference data is too old to use RTK technique. The L1 ambiguities were used to initialize a PPP filter, in 1 epoch. A careful cycle slip detection was performed using Doppler measurements.

3.7.2 POSITIONING WITH GRAPHIC PSEUDORANGES

First, the unambiguous GRAPHIC pseudorange was used directly, instead of code measurements as explained in 3.5. The result can be found on Figure 5. It can be seen that the amplitude of the error is divided by 2, as expected from noise propagation law.

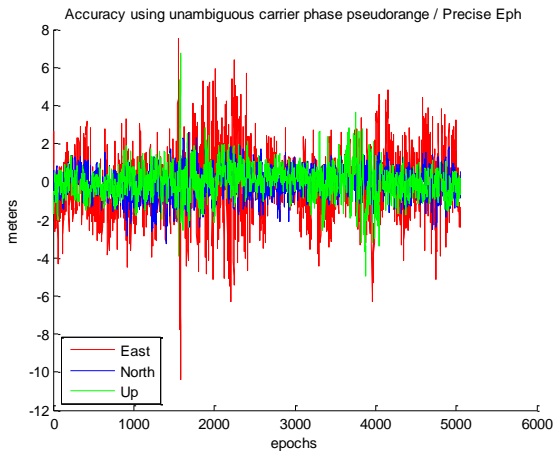


Figure 5 Positioning error using only GRAPHIC unambiguous pseudorange and IGS rapid ephemerides on a uBlox LEA-6T. Pseudoranges were weighed by the cosecant function of the elevation

angle. Data rate is 1/5 Hz. No assumption was made on the receiver dynamic.

Although the error is divided by 2, the positioning accuracy is still relatively low on the uBlox receiver (meter-level), due to the high level of noise and multipath on code measurement and since no assumption was made on the receiver dynamic. One way to improve it would be to smooth the unambiguous GRAPHIC pseudorange. The smoothing can be performed using observations obtained before the communication link loss and must be continued after. A first idea would be to use a Hatch filter with the ambiguous L1 carrier-phase smoothing the code pseudorange. However, the Hatch filter has to be reinitialized every time a cycle clip occurs. Moreover, it can bias measurements because of the ionospheric divergence issue. A more robust method is proposed in the following section.

3.7.3 ESTIMATING THE IONOSPHERIC DELAY IN THE PPP FILTER: THE PHASE/CMC PPP FILTER

Another method proposed in this paper is to estimate carrier-phase ionospheric delay obtained using code and unambiguous carrier-phase measurements and to subtract from unambiguous carrier-phase measurements, i.e. :

$$\left\{ \begin{array}{l} \frac{\overline{\Phi_1 - P_1}}{2} = I_{\Phi_1} + b_{r, \frac{\overline{\Phi_1 - P_1}}{2}} - b_{\frac{\overline{\Phi_1 - P_1}}{2}}^s + m_{\frac{\overline{\Phi_1 - P_1}}{2}} + \varepsilon_{\frac{\overline{\Phi_1 - P_1}}{2}} \\ \overline{\Phi_1} = \rho + c(dt_{P_{IF}} - dT_{P_{IF}}) + I_{\Phi_1} + T + b_{r, \Phi_1} - b_{\Phi_1}^s + W\lambda_1 + m_{\Phi_1} + \varepsilon_{\Phi_1} \end{array} \right.$$

This filter was nicknamed Phase/CMC PPP filter, as it uses phase and “code minus carrier” (CMC) observations. The method is inspired from [Muellerschoen, et al., 2004], which uses a linear fit instead of a Kalman filter and was suggested by Denis Laurichesse from CNES. A Kalman filter is used to estimate $I_{\Phi_1} - b_{\frac{\overline{\Phi_1 - P_1}}{2} - P_{IF}}^s$ from $\frac{\overline{\Phi_1 - P_1}}{2}$ observable (independently on each satellite) together with the position, tropospheric delay, and remaining unknown ambiguities. More details are given on that Kalman filter in the Annex. $b_{r, \frac{\overline{\Phi_1 - P_1}}{2} - P_{IF}}$ is estimated as a receiver clock term, biasing all measurements. A sigma of 5 meters per hour is assumed in the process noise of the Kalman filter for $I_{\Phi_1} - b_{\frac{\overline{\Phi_1 - P_1}}{2} - P_{IF}}^s$, while $b_{r, \frac{\overline{\Phi_1 - P_1}}{2} - P_{IF}}$ is not constrained. This smoothing method is a lot more robust to short period loss of locks and data outages that can be encountered by a road user.

It is interesting to denote that the pseudorange $\overline{\Phi_1} - \frac{\overline{\Phi_1 - P_1}}{2}$ is affected by the same satellite bias as the unambiguous GRAPHIC pseudorange as long as the satellite bias is constant in the smoothing window, which turned out to be the case in practice.

A plot of the positioning accuracy obtained can be found on Figure 6.

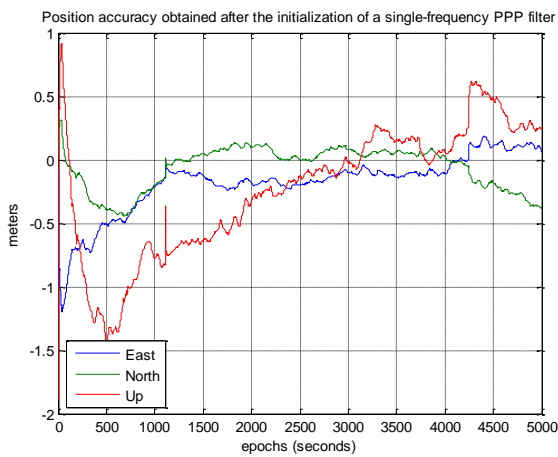


Figure 6 Positioning error on a uBlox LEA-6T obtained while using a Kalman filter estimating ionospheric delays on each satellite, position, tropospheric delays and remaining ambiguities. The PHASE/CMC PPP filter was initialized with 8 ambiguities (out of 9 visible satellites) at the first epoch. Data comes from the same collection, but rate was kept at 1Hz, to ease Doppler cycle slip detection. Pseudoranges were weighted by the cosecant function of the elevation angle. No assumption was made on the dynamic of the receiver.

A convergence time can clearly be seen on the figure. It is the time required to obtain a smoothed ionospheric delay estimation. Note that the PHASE/CMC PPP filter can be run on the rover in parallel of RTK positioning when data from the reference station is available, so that a sub-meter level position could be obtained directly when the communication link is lost. The filter was tried with and without residual tropospheric delay estimation. It turns out that the estimation of tropospheric delay was not necessary provided UNB3m [Leandro, et al., 2006] prediction model was used, as it extended convergence time

3.7.4 POSITIONING WITH UNAMBIGUOUS CARRIER-PHASE AND EGNOS IONOSPHERIC CORRECTIONS

It has been shown in 3.6 that unambiguous carrier-phase could be used for positioning together with broadcasted ephemeris, provided its specific bias is correctly taken into account. The same Kalman filter as in 3.7.3 was used to estimate the position. The observation vector contains L1 carrier phase only measurements together with EGNOS ionospheric corrections instead of code-minus-phase observations. EGNOS ionospheric corrections were weighted with the standard deviation of the ionospheric slant delay computed as recommended in [RTCA, 2006]. One issue is that the EGNOS ionospheric correction is not affected by a random noise error on a short-term window. Then, the Kalman filter may give too much confidence in the estimated ionospheric delay. The process noise of the estimated ionospheric delay was set to a very high value, so that its covariance matrix doesn't become overly optimistic. Tropospheric delay was not estimated, as it

turned out to weaken the model. UNB3m predicted tropospheric delay was used instead. The positioning error is plot on Figure 7.

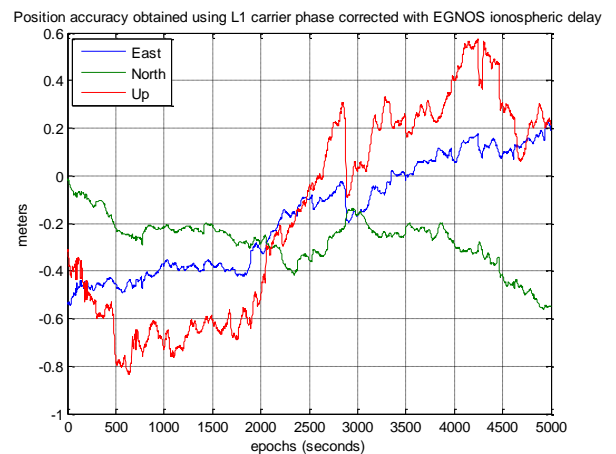


Figure 7 Positioning error obtained using L1 carrier phase corrected with EGNOS ionospheric delay and precise ephemeris. Pseudoranges were weighted using broadcasted variance of ionospheric slant delay error. Data rate was 1Hz. No assumption was made on the receiver dynamic.

The positioning accuracy obviously highly depends on EGNOS corrections accuracy, which are at the meter level. The accuracy of satellite biases is also very important, as it is multiplied by 2 (see 3.6).

3.7.5 POSITIONING WITH UNAMBIGUOUS DUAL-FREQUENCY CARRIER-PHASE

Finally, the algorithm is tested using dual-frequency data of a Novatel receiver connected to the same antenna than the uBlox. Centimeter-level position was expected [Laurichesse, et al., 2009]. However, the resulting accuracy was a little lower than expected. It can be due to the fact that position was not constrained and that biases required for the processing (see 3.4) may introduce decimeter-level error. However, 10-cm accuracy was obtained in horizontal.

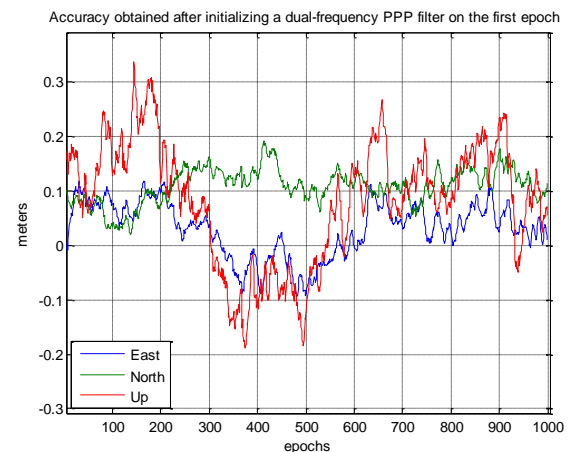


Figure 8 Positioning error obtained after initializing a dual-frequency PPP filter with 8 satellite narrowlane ambiguities out of 9 visible. Receiver was a Novatel ProPak-G2 dual-frequency receiver. Data was collected at 1/5Hz. No

assumption was made on the receiver dynamic. Earth tides and ocean loading were not modeled.

4. REDUCING REFERENCE RECEIVER CODE NOISE AND MULTIPATH CONTRIBUTION IN THE AMBIGUITY FLOAT SOLUTION

Carrier-phase tracking is less robust than code tracking. In difficult environment, receivers will experience frequent cycle slips, i.e. changes of ambiguities value and complete loss of tracking. In these conditions, urban users have to fix ambiguities almost as soon as carrier-phase observables are available. [Kubo, et al., 2007] and [Bahrami, et al., 2010] recommend to use instantaneous ambiguity resolution to avoid using cycle slip detection algorithm which are not always reliable and are a burden on real-time processing. To fix ambiguities instantaneously, the float solution obtained using code and carrier-phase measurement has to be as precise as possible. The influence of code accuracy on single-epoch ambiguity fixing success rate was studied in [Milbert, 2005]. It is shown that the success rate highly depends on the accuracy of the estimated float ambiguities. To improve the accuracy of these float ambiguities, different techniques can be found in the literature: Doppler smoothing in the observation or the position domain [Bahrami, et al., 2010] and [Kubo, et al., 2008], INS integration [Petovello, 2003]... The approach presented in this paper is to reduce the level of noise and multipath of the code double difference. Considering that it is composed of both noise and multipath from the reference receiver and from the rover receiver, a first step is to reduce the contribution of the reference receiver. Although it is usually smaller than rover receiver contribution, reference receiver noise and multipath can be at decimeter level if the code measurements are smoothed and at meter level if not.

A method was proposed by the authors to reduce the noise and multipath contribution of the reference receiver to centimeter-level (widelane carrier-phase noise level) [Carcanague, et al., 2011]. The algorithm presented was based on 3 steps:

- First, the widelane ambiguities were estimated on the reference receiver, using widelane satellite biases available from PPP-Wizard project website [CNES, 2011] or IGS GRGS analysis center [Perosanz, et al., 2009]. The estimated widelane ambiguities are then added to widelane carrier phase to obtain unambiguous widelane carrier-phase measurements.
- Unambiguous widelane carrier phase measurements is then differenced with rover narrowlane code measurements. Satellite biases present in the resulting measurements are removed using PPP-AR products.
- RTK positioning can then be performed classically, using single-differenced or double-differenced observables indifferently.

This method has the advantage to improve the accuracy of the ambiguities float solution (and of code differential positioning) up to a factor of $\sqrt{2}$ if the reference receiver and the rover have similar level of noise. It was also shown that position could be obtained, using single-differenced instead of double-differenced observables used in classic RTK technique. In single-differenced observables, ambiguities are not as correlated as in double-differenced observables [Enge, et al., 2nd Edition]. Furthermore, RTK with single difference measurements avoids the issues related to reference satellite choice (and switch) in the ambiguity values and the positioning filter covariance matrix. However, the use of single-difference showed little improvements in the ambiguity resolution success rate, mainly due to the difficulty associated to the estimation of the additional hardware bias required [Carcanague, et al., 2011].

In this section, the concept of using only unambiguous carrier-phase observables from the reference station instead of code pseudorange will be extended to single-frequency receivers.

4.1 SINGLE-FREQUENCY CASE

Just as in the case of the algorithm presented in [Carcanague, et al., 2011], the aim is to use only unambiguous carrier-phase measurements from the reference receiver instead of code measurements, in a short-baseline scenario.

Contrary to the dual-frequency case, no combination can be performed so that ionospheric delay on the carrier phase combination of the reference receiver equals ionospheric delay on the code combination of the rover. One way to remove the ionospheric delay is to use the GRAPHIC combination [Laurichesse, et al., 2009], with the carrier phase of the reference receiver and the code of the rover. Let's write the code and carrier phase measurements on the reference and the rover receiver, in the case of a short baseline (atmospheric delay are the same on the rover and the reference station):

$$\begin{cases} \phi_1^{\text{ref}} = \rho^{\text{ref}} + c(dt^{\text{ref}} - dT) + T - I_1 + N_1^{\text{ref}} \lambda_1 + b_{r,\phi_1^{\text{ref}}} - b_{\phi_1^s} + \varepsilon_{\phi_1} \\ P_1^{\text{ref}} = \rho^{\text{ref}} + c(dt^{\text{ref}} - dT) + T + I_1 + b_{r,P_1^{\text{ref}}} - b_{P_1^s} + \varepsilon_{P_1^{\text{ref}}} \end{cases}$$

$$\begin{cases} \phi_1^{\text{rov}} = \rho^{\text{rov}} + c(dt^{\text{rov}} - dT) + T - I_1 + N_1^{\text{rov}} \lambda_1 + b_{r,\phi_1^{\text{rov}}} - b_{\phi_1^s} + \varepsilon_{\phi_1} \\ P_1^{\text{rov}} = \rho^{\text{rov}} + c(dt^{\text{rov}} - dT) + T + I_1 + b_{r,P_1^{\text{rov}}} - b_{P_1^s} + \varepsilon_{P_1^{\text{rov}}} \end{cases}$$

The proposed single-frequency algorithm is as such:

- **(1) Resolution of the L1 ambiguity on the reference receiver.** The method described in 2.2 can be used. To fasten the resolution, the coordinates of the reference station can be surveyed and assumed known.
- **(2) Combinations using the unambiguous carrier phase measurements of the reference receiver and the code measurements of the rover.** Two observables are created in this step:
 - The first is a single difference (between receivers) of the L1 carrier phase observables.
 - The second is the GRAPHIC combination, with the unambiguous

phase measurements of the reference receiver and the code measurements of the rover, i.e.:

$$\begin{cases} \frac{\overline{\phi_1^{\text{ref}} + P_1^{\text{rov}}}}{2} = \frac{\rho^{\text{ref}} + \rho^{\text{rov}}}{2} + c(dt_1 - dT) + T + b_{r, \frac{\phi_1^{\text{ref}} + P_1^{\text{rov}}}{2}} - b_{\frac{\phi_1 + P_1}{2}}^s + \varepsilon_{\frac{\phi_1^{\text{ref}} + P_1^{\text{rov}}}{2}} \\ \frac{\phi_1^{\text{ref}} - \phi_1^{\text{rov}}}{2} = \frac{\rho^{\text{ref}} - \rho^{\text{rov}}}{2} + c \cdot dt_2 + b_{r, \frac{\phi_1^{\text{ref}} - \phi_1^{\text{rov}}}{2}} + (N_1^{\text{ref}} - N_1^{\text{rov}})\lambda_1 + \frac{\varepsilon_{\Delta\phi}}{2} \end{cases}$$

With $\overline{\phi_1^{\text{ref}}} = \phi_1^{\text{ref}} - N_1^{\text{ref}}\lambda_1$, $dt_1 = dt^{\text{ref}} + dt^{\text{rov}}$ and $dt_2 = dt^{\text{ref}} - dt^{\text{rov}}$

- **(3) Differencing between 2 satellites to eliminate clock and receiver bias terms.**

i.e.:

$$\begin{cases} \nabla \frac{\overline{\phi_1^{\text{ref}} + P_1^{\text{rov}}}}{2} = \nabla \frac{\rho^{\text{ref}} + \rho^{\text{rov}}}{2} + c \cdot \nabla dT + \nabla T^{\text{ref}} - \nabla b_{\frac{\phi_1 + P_1}{2}}^s + \varepsilon_{\frac{\phi_1^{\text{ref}} + P_1^{\text{rov}}}{2}} \\ \frac{\nabla \Delta \phi_1}{2} = \frac{\nabla \Delta \rho}{2} + \nabla \Delta N \cdot \frac{\lambda_1}{2} + \frac{\varepsilon_{\nabla \Delta \phi_1}}{2} \end{cases}$$

The operator ∇ represents the between-satellite difference. If the reference receiver is single-frequency, a precise positioning system can be obtained by removing the single-differenced geometric range from reference receiver to satellite, the single-differenced satellite clock and the single-differenced tropospheric delay. However, if the reference receiver is dual-frequency, the last step can be applied:

- **(4) Removing single-differenced unambiguous ionosphere-free carrier-phase measurements from the reference receiver.**

$$\begin{cases} \nabla \frac{\overline{\phi_1^{\text{ref}} + P_1^{\text{rov}}}}{2} - \nabla \phi_{\text{IF}} = -\frac{\nabla \Delta \rho}{2} - \nabla b_{\frac{\phi_1 + P_1}{2} - \phi_{\text{IF}}}^s + \varepsilon_{\frac{\phi_1^{\text{ref}} + P_1^{\text{rov}}}{2}} \\ \frac{\nabla \Delta \phi_1}{2} = \frac{\nabla \Delta \rho}{2} + \frac{\varepsilon_{\nabla \Delta \phi_1}}{2} \end{cases}$$

Where $\overline{\phi_{\text{IF}}} = \phi_{\text{IF}} - \beta N_{\text{WL}} - N_1 \lambda_{\text{NL}}$

Different techniques can be used to estimate $b_{\frac{\phi_1 + P_1}{2} - \phi_{\text{IF}}}^s$ for each satellite. Three techniques are described in 3.5.

We see that the position of the rover can be estimated once again accurately, using a precise ambiguous measurement and a coarse unambiguous measurement that doesn't introduce reference receiver code noise.

4.2 TEST ON REAL DATA

This algorithm was tested on 2 IGS stations (USNO and USN3). The ambiguities were estimated on USNO using a dual-frequency PPP filter. The results can be found in Table 2.

Table 2 Estimated baseline accuracy comparison, using classic P1 code double difference and the technique described in 4.1.

	Classic code double difference	GRAPHIC with USNO unambiguous carrier phase and USN3 code measurements
Standard deviation (X,Y,Z meters)	0.47/0.90/0.70	0.36/0.66/0.52

Mean (X,Y,Z meters)	-0.01/0.04/0.01	-0.01/0.00/0.02
---------------------	-----------------	-----------------

Since both stations have similar level of code noise and multipath, the final position accuracy is improved by a ratio close to $\sqrt{2}$, as expected from noise propagation law. However, this algorithm is not really interesting in the case of dual-frequency reference receivers, which usually have state-of-the-art tracking loop and code smoothing techniques that results in decimeter level L1 C/A code noise and multipath. A more interesting application of this algorithm is the single-frequency reference receiver case. Indeed, the algorithm could be used on a low-cost receiver that would be used as a reference receiver. Instead of using code measurements that have a noise superior to 2 meters (1σ [Realini, 2009]), the unambiguous carrier-phase would be used, together with estimated tropospheric delay and precise satellite clock and orbits. The main application of this technique would be first to extend the spatial range of a reference dual-frequency receiver (limited to 10km to avoid atmospheric errors) with a low cost receiver situated closer to the rover, or secondly to use a low-cost receiver as a reference receiver. In the first case, the ambiguities of the low cost receiver could be instantly determined using the technique explained in 3. In the second case, the ambiguities would have to be estimated as in [Laurichesse, et al., 2009] or using a PPP filter. This technique acts as a long term smoothing using PPP ambiguities, but contrary to classic smoothing techniques affected by ionospheric divergence, the longer the window, the better the accuracy. Indeed in a PPP filter, the longer the time window, the better the ambiguity accuracy.

An example of improvement in term of code solution accuracy can be found in Table 1. In that case, uBlox ambiguities were instantaneously initialized using undifferenced ambiguities from TLSE and RTK between the 2 stations.

In Table 4, the ambiguities were estimated on the uBlox, using a real-time-like processing. A single-frequency PPP filter was used, using EGNOS corrections. The uBlox code measurements were not used at all in the processing. TGD, UNB3m tropospheric delay and IGS final clock were removed from measurements, to obtain double-differenced geometric range (see step (3) of 4.1). It can be seen that the contribution of the reference uBlox in the RTK initial float solution residuals is reduced to decimeter level. To estimate ambiguities on the reference station, the best method with a low-cost receiver turned out to be the EGNOS-based PPP filter in our test, as the wavelength associated to the estimated ambiguities is 2 times the wavelength of the GRAPHIC combination. To form the GRAPHIC combination with the code of the rover and the unambiguous carrier phase of the reference receiver, the reference receiver ambiguity estimated with EGNOS-based PPP filter is divided by 2 and so is the error associated to it.

Table 3 Noise+multipath statistics of the 2 techniques in a test between a uBlox LEA-6T and TLSE IGS station, instantaneously initializing uBlox ambiguities with TLSE ambiguities and known double differenced ambiguities.

	Classic smoothed code double difference	GRAPHIC with uBlox unambiguous carrier phase and TLSE code measurements (instantaneous initialization of ambiguities, see 3.2)
Standard deviation	1.22m	0.34m
Mean	-0.05m	-0.01m

Table 4 Noise+multipath statistics of the technique in a test between a uBlox LEA-6T and TLSE IGS station, estimating ambiguities with a single-frequency EGNOS-based PPP filter.

	Classic smoothed code double difference	GRAPHIC with uBlox unambiguous carrier phase and TLSE code measurements (Ambiguities are estimated using a PPP filter, see 3.2)
Standard deviation	1.22m	0.45m
Mean	-0.07m	-0.03m

This technique can allow lower-cost single-frequency receivers to be used as reference stations.

5. CONCLUSION AND FUTURE WORK

In this paper, it is shown that estimating the carrier-phase ambiguities on the reference receiver can allow 2 important improvements for a RTK road user:

- PPP ambiguities of the rover can be instantly initialized using the technique described in 3. . The PPP filter can be used if the reference station data is no longer available. Decimeter level accuracy for dual-frequency users and a few decimeter precision (with a low-cost receiver) for single-frequency users were demonstrated in a static case. A single-frequency PPP filter that can use either EGNOS ionospheric corrections or code-based ionospheric observations was presented in this paper. Three methods were presented to estimate the necessary satellite biases.
- Secondly, it has been shown that once ambiguities are determined on the reference receiver, a new unambiguous positioning method can be used for single-frequency users using only unambiguous carrier-phase measurements of the reference receiver, together with predicted tropospheric delay, satellite clocks and orbits which accuracy are usually at decimeter-level in

real-time. This method is especially recommended for low-cost single-frequency receivers used as reference stations as it can completely avoid the use of reference receiver code measurements.

However, a number of improvements remain to be done. First, the estimation of satellite biases would be more accurate using a network of receivers. Secondly, the accuracy of the single-frequency PPP filter highly depends on the accurate cycle slips detection. Doppler measurements were used in this paper, but low-cost INS can be used as well [Takasu, et al., 2008]. Finally, phase measurements were used with either code measurements or EGNOS corrections in our single-frequency PPP filter. Using the 3 observations altogether in a unique single-frequency PPP filter could be an idea to reduce convergence time while keeping a high level of precision of the final solution.

ACKNOWLEDGMENTS

The authors would like to thank Denis Laurichesse for his advices on the use of the PPP-AR satellite clock products, his idea on smoothing the ionospheric delay in the Kalman filter in the case of single-frequency PPP as well as the login/password to the real-time CNES Ntrip caster. The authors are also thankful to the ENAC Paparazzi team for the loan of the uBlox receiver as well as the Association Nationale de la Recherche et de la Technologie (ANRT) and CNES for the financial support.

BIBLIOGRAPHY

- Bahrami, M., & Ziebart, M. (2010). *Instantaneous Doppler-Aided RTK Positioning with Single Frequency Receivers*. IEEE.
- Banville, S., & Langley, R. B. (2009). *Improving Real-Time Kinematic PPP with Instantaneous Cycle-Slip Correction*. ION GNSS: 22nd International Meeting of the Satellite Division of The Institute of Navigation, Savannah, GA, September 22-25, 2009.
- Banville, S., & Tang, H. (2010). *Antenna Rotation and Its Effects on Kinematic Precise Point Positioning*. ION GNSS : 23rd International Technical Meeting of the Satellite Division of The Institute of Navigation, Portland, OR, September 21-24, 2010.
- Banville, S., Santerre, R., Cocard, M., & Langley, R. B. (2008). *Satellite and Receiver Phase Bias Calibration for Undifferenced Ambiguity Resolution*. ION NTM 2008, 28-30 January, San Diego, CA.
- Bisnath, S., & Gao, Y. (2009). *Current State of Precise Point Positioning and Future Prospects and Limitations*. M.G. Sideris (ed.), Observing our Changing Earth, International Association of Geodesy Symposia 133, Springer-Verlag Berlin Heidelberg 2009.

- Carcanague, S., Julien, O., Vigneau, W., & Macabiau, C. (2011). *A New Algorithm for GNSS Precise Positioning in Constrained Area*. Proceedings of ION International Technical Meeting, January 24-26, San Diego, CA.
- CNES. (2011). *The PPP-Wizard Project*. Consulté le June 27, 2011, sur <http://www.ppp-wizard.net/index.html>
- Collins, J. P. (1999). *An overview of GPS inter-frequency carrier phase combinations*. UNB, Department of Geodesy and Geomatics.
- Collins, P. (2008). *Isolating and estimating undifferenced GPS integer ambiguities*. ION NTM 2008, 28-30 January 2008, San Diego, CA.
- de Jonge, P. J., Bock, Y., & Bevis, M. (2000). *Epoch-by-Epoch™ Positioning and Navigation*. Proceedings of ION GPS-2000, The Institute of Navigation, Alexandria, VA, pp. 337-342, 2000.
- Dow, J., Neilan, R. E., & Rizos, C. (2009). *The International GNSS Service in a changing landscape of Global Navigation Satellite Systems*. Journal of Geodesy, 83:191–198, DOI: 10.1007/s00190-008-0300-3.
- Enge, P., & Misra, P. (2nd Edition). *GLOBAL POSITIONING SYSTEM Signals, Measurements, and Performance*.
- Ge, M., Gendt, G., Rothacher, M., Shi, C., & Liu, J. (2008). *Resolution of GPS Carrier-phase Ambiguities in Precise Point Positioning (PPP) with Daily Observations*. Journal of Geodesy, Vol. 82, No. 7, pp. 389-399.
- Geng, J., Meng, X., Dodson, A. H., Ge, M., & Teferle, F. N. (2010). *Rapid re-convergences to ambiguity-fixed solutions in precise point positioning*. Springer.
- Henkel, P., & Günther, C. (2007). *Three frequency linear combinations for Galileo*. Hannover, Germany: Proc. of 4-th IEEE Workshop on Positioning, Navigation and Communication (WPNC '07).
- Henkel, P., Gomez, V., & Gunther, C. (2009). *Modified LAMBDA for absolute carrier phase positioning in the presence of biases*. ION GNSS 2009, 22nd International Meeting of the Satellite Division of The Institute of Navigation, Savannah, GA, September 22-25, 2009.
- Kubo, N., & Pullen, S. (2008). *Instantaneous RTK Positioning Based on User Velocity Measurements*. ION GNSS.
- Kubo, N., & Yasuda, A. (2007). *Instantaneous RTK Positioning with Altitude-aiding for ITS Application*. ION GNSS 2007 20th International Technical Meeting of the Satellite Division, 25-28, September 2007, Fort Worth, TX.
- Laurichesse, D., Mercier, F., & Berthias, J. (2009). *Zero-difference integer ambiguity fixing on single frequency receivers*. ION GNSS.
- Laurichesse, D., Mercier, F., Berthias, J., Broca, P., & Cerri, L. (2009). *Integer Ambiguity Resolution on Undifferenced GPS Phase Measurements and its Application to PPP and Satellite Precise Orbit Determination*. Navigation, Journal of the institute of Navigation, Vol. 56, N° 2, Summer 2009.
- Leandro, R. F. (2009). *Precise Point Positioning with GPS: A New Approach for Positioning, Atmospheric Studies, and Signal Analysis*. PhD thesis, Department of Geodesy and Geomatics Engineering, Technical Report No. 267 University of New Brunswick, Fredericton, New Brunswick, Canada, 232 pp.
- Liu, J. (2003). *Resolution Strategies in Single and Multiple Reference Station Scenarios*. MSc thesis, UCGE Reports Number 20168, Department of Geomatics Engineering, University of Calgary.
- Loyer, S., Pérosanz, F., Capdeville, H., & Mercier, F. (2010). *CNES-CLS IGS Analysis Center : Results and processing strategies*. Marne-La-Vallée: REFAG.
- Melbourne, W. (1985). *The Case for Ranging in GPS Based Geodetic System*. Proceedings of 1st International Symposium on Precise Positioning with the Global Positioning System, edited by Clyde Goad, U.S. Department of Commerce, Rockville, Maryland, 15-19 April.
- Milbert, D. (2005). *Influence of Pseudorange Accuracy on Phase Ambiguity Resolution in Various GPS Modernization Scenarios*. NAVIGATION, Spring 2005, 52(1), pp.29-38.
- Odjik, D. (2008). *What does "geometry-based" and "geometry-free" mean in the context of GNSS?* GNSS Solution, Inside GNSS, March/April 2008.
- Olynik, M. C. (2002). *Temporal Characteristics of GPS Error Sources and Their Impact on Relative Positioning*. MSc, University of Calgary, Department of Geomatics Engineering.
- Petovello, M. G. (2003). *Real-Time Integration of a Tactical-Grade IMU and GPS for High-Accuracy Positioning and Navigation*. University of Calgary, PhD thesis.

Realini, E. (2009). *goGPS free and constrained relative kinematic positioning with low cost receivers*. PhD thesis, Politecnico Di Milano.

RTCA. (2006). *Minimum Operational Performance Standards for Global positioning System/Wide Area augmentation System Airborne Equipment*.

Takasu, T. (2009). *RTKLib: Open Source Program Package for RTK-GPS*. Tokyo: FOSS4G.

Takasu, T., & Yasuda, A. (2008). *Cycle Slip Detection and Fixing by MEMS-IMU/GPS Integration for Mobile Environment RTK-GPS*. ION GNSS.

Teunissen. (2001). *Integer estimation in the presence of biases*. Journal of Geodesy, pp. 399-407, Springer, 2001.
Teunissen, P. (1993). *Least-squares estimation of the integer GPS ambiguities*. Invited lecture, Section IV Theory and Methodology, IAG General Meeting, Beijing, China, August.

Teunissen, P., & Kleusberg, A. (1998). *GPS for Geodesy*. 2nd enlarged edition, Springer Verlag.

Urquhart, L. (2009). *An Analysis of Multi-Frequency Carrier Phase Linear Combinations for GNSS*. Senior technical report, Department of Geodesy and Geomatics Engineering Technical Report No. 263, University of New Brunswick, Fredericton, New Brunswick, Canada, 71 pp.

Wu, F., Kubo, N., & Yasuda, A. (2003). *Fast Ambiguity resolution in RTK-GPS Positioning for Marine Navigation*. Proceedings of ION NTM 2003, Anaheim, California, 22-24 January 2003.

Wübbena, G. (1985). *Software Developments for Geodetic Positioning with GPS Using TI 4100 Code and Carrier Measurements*. Proceedings of 1st International Symposium on Precise Positioning with the Global Positioning System, edited by Clyde Goad, U.S. Department of Commerce, Rockville, Maryland, 15-19 April, pp. 403-412.

Yang, L., Hill, C., & Moore, T. (2010). *Implementation of Wide Area Broadcast NRTK on a Communication Satellite Platform*. 23rd International Technical Meeting of the Satellite Division of The Institute of Navigation, Portland, OR, September 21-24, 2010.

ANNEXE

1. KALMAN FILTER DESCRIPTION FOR 3.7.3

a. State vector

The state vector X is as such:

$$X = \begin{bmatrix} X \\ Y \\ Z \\ dt \\ ztd \\ I_1 \\ \vdots \\ I_n \\ dt_{iono} \\ N_1 \\ \vdots \\ N_{n_1} \end{bmatrix}$$

Where

- X, Y, Z are the receiver antenna ECEF coordinates
- dt is the estimated receiver clock (including hardware bias)
- ztd is the estimated residual tropospheric delay
- I_i is the estimated ionospheric delay for satellite i
- n is the total number of satellites
- dt_{iono} is the ‘ionospheric clock’, which is the term common to all estimated ionospheric delays
- N_i are the ambiguities that have not been initialized (from satellites with unknown reference receiver ambiguities or that have first been tracked after initialization)
- n_1 is the number of ambiguities that have not been initialized.

The estimation of dt_{iono} is necessary so that the value of the ionospheric delay remains the same after a loss of lock or after a change of the reference satellite, as all ionospheric delay observables are offset with a common ambiguity.

b. Observation vector

The observation vector is as such:

$$Z = \begin{bmatrix} \underbrace{\begin{bmatrix} \overline{\phi_1^1} \\ \vdots \\ \overline{\phi_1^{n_2}} \\ \frac{\overline{\phi_1^1} - p_1^1}{2} \\ \vdots \\ \frac{\overline{\phi_1^{n_2}} - p_1^{n_2}}{2} \end{bmatrix}}_{\text{satellites with known ambiguities}} \\ \underbrace{\begin{bmatrix} \phi_1^{n_2+1} \\ \vdots \\ \phi_1^n \\ \frac{\phi_1^{n_2+1} - p_1^{n_2+1}}{2} \\ \vdots \\ \frac{\phi_1^n - p_1^n}{2} \end{bmatrix}}_{\text{satellites with unknown ambiguities}} \end{bmatrix}$$

Where

- $n_2 = n - n_1$ is the number of satellites with known ambiguities

c. Transformation matrix

The transformation matrix H is as such:

$$H = \begin{bmatrix} \begin{bmatrix} 1 \\ H_{n_2} \vdots M(e_{n_2}) \\ 1 \end{bmatrix} & \begin{bmatrix} -\mathbb{I}_{n_2} & 0 \\ 0 & 0 \end{bmatrix} & \begin{bmatrix} 0 & 0 & 1 \\ 0 & 0 & \vdots \\ 1 & 0 & 0 \end{bmatrix} \\ \begin{bmatrix} 1 \\ H_{n_1} \vdots M(e_{n_1}) \\ 1 \end{bmatrix} & \begin{bmatrix} 0 & 0 \\ 0 & -\mathbb{I}_{n_1} \end{bmatrix} & \begin{bmatrix} 0 & \mathbb{I}_{n_1} \\ 0 & 0 \end{bmatrix} \\ \begin{bmatrix} 0 & 0 & 0 \\ 0 & 0 & 1 \\ 0 & \mathbb{I}_{n_1} & \vdots \\ 0 & 1 & \frac{-\mathbb{I}_{n_1}}{2} \end{bmatrix} \end{bmatrix}$$

Where:

- H_{n_1} and H_{n_2} are the geometrical matrix of the satellites with unknown ambiguities and known ambiguities respectively.
- $M(e_{n_i})$ is the tropospheric mapping function for the elevation of the satellites with unknown ambiguities and known ambiguities respectively.
- \mathbb{I}_{n_i} is the identity matrix of size n_i .